

STEADY STATE ANALYSIS AND MODELLING OF A SERIES ACTIVE POWER FILTER

RAFAEL R. MATIAS*, CURSINO B. JACOBINA*, ALEXANDRE C. OLIVEIRA*, EDISON R. C. DA SILVA*, LUCAS V. HARTMANN*, WELFLEN RICARDO N. SANTOS*

*Unidade Acadêmica de Engenharia Elétrica
Universidade Federal de Campina Grande (UFCG-PB)
58.109-970 Av. Aprígio Veloso, 882
Campina Grande - Paraíba, Brasil

Emails: [rafaelrocha@dee.ufcg.edu.br, jacobina@dee.ufcg.edu.br, aco@dee.ufcg.edu.br, edison@dee.ufcg.edu.br, lucas.hartman@gmail.com, welflen@gmail.com]

Abstract— This paper presents a steady state analysis and modelling of a three-phase series active power filter. In this study, a simple way to obtain the transfer function of load voltage is shown, allowing new transfer functions to be easily obtained in case structure changes. The steady state analysis allows to know the the source power factor as well as behavior of the fundamental component of currents and voltages. From this analysis it is shown that in some conditions it is possible, in some cases, to regulate the load voltage and reduce the harmonics voltages, without an extra dc-link source. A suitable control strategy that regulates the load voltage and minimizes the voltage harmonics simultaneously is presented. Simulated results of steady state and dynamic operation are presented.

Keywords— Series active filter, steady state, modelling.

I. INTRODUCTION

The increase of electrical pollution causes a disturbance in the sinusoidal waveforms of voltage and current in electrical system. Consequently, power losses increase and the electrical equipment works inadequately. The electrical power quality has recently become an important technical issue, thus stimulating the use active power compensation schemes [1, 2]. The distortion of the sinusoidal waveform is mainly produced by non-linear loads, and is propagated as voltage and current harmonics to the whole system. Another problem to be considered is the variation of the bus voltage amplitude (source voltage), which occurs when a load block or a generator is connected or disconnected in electrical system, for example.

The series active power filter (SAPF) [3, 4, 5] provides load voltage control, which eliminates voltage disturbances, such as sags, notches, flickers and voltage harmonics, so that there exists only the fundamental load voltage component with constant magnitude in the system. The SAPF is implemented by using an electronic power converter connected to a transformer located between the source and the load, as shown in Fig. 1.

This paper presents a study of characteristics of such

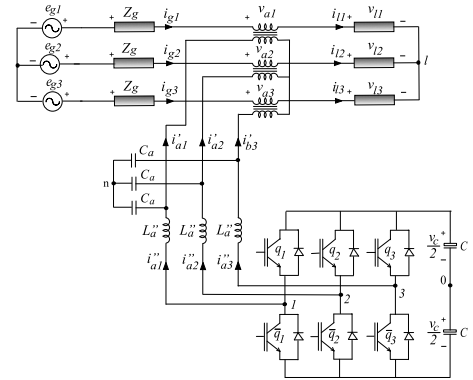


Fig. 1: Three-phase series active power filter.

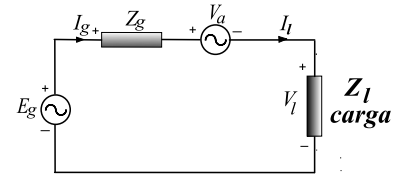


Fig. 2: Single-phase ideal series active power filter model.

system. The system is modelled, and a steady state analysis is done, in which the behavior of currents, voltages and source power factor are investigated. The objective is to minimize losses due to the converter switching and verify the operation intervals in which the source power factor is improve or not. The steady state analysis also shows that it is possible to regulate the load voltage without any external source, in some cases, thus the SAPF is not only used as a harmonic filter. Differently from the common case found in the literature, but also as a load voltage regulator.

II. SAPF MODEL

Modelling of SAPF begin with a simple ideal circuit (Fig. 2). The load voltage transfer function is then determined for this circuit, and other components are added to the model, step by step. This way, flexibility for structure change is obtained. From the circuit shown in Fig. 2, the following equations can be written:

$$\mathbf{E}_g = \mathbf{V}_a + \mathbf{Z}_g \mathbf{I}_g + \mathbf{I}_l \mathbf{Z}_l \quad (1)$$

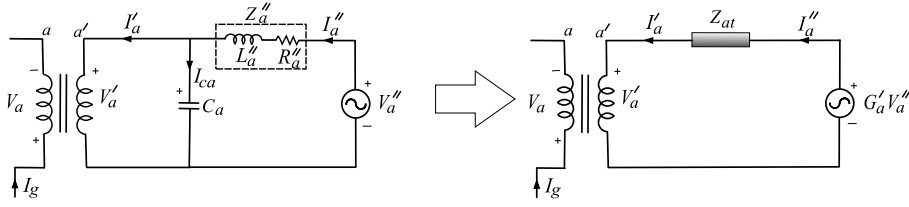


Fig. 3: RLC filter model and transformer of SAPF.

$$\mathbf{I}_l = \mathbf{I}_g = \frac{\mathbf{V}_l}{Z_l} = \mathbf{V}_l(a_l + jb_l) \quad (2)$$

in which a linear load is used. Substituting (2) into (1) allows easily obtaining a simplified load voltage transfer function:

$$\mathbf{V}_l = -\frac{Z_l}{Z_g + Z_l} \mathbf{V}_a + \frac{Z_l}{Z_g + Z_l} \mathbf{E}_g \quad (3)$$

To complete the model containing all elements of Fig. 1 (the converter is modelled by a voltage source and switches are not included in the model), it is necessary to add models for the transformer and the converter passive harmonic filter. With this purpose, the Thevenin-Norton theorem is used to obtain an equation where the voltage v_{aj} ($j = 1, 2, 3$) is a function of the converter voltage v''_{aj} , in the circuit shown in Fig. 3 (from now on the subscript j will be omitted).

From Thevenin-Norton theorem the primary transformer voltage v'_a can be written as a function of v''_a :

$$\mathbf{V}'_a = G'_a \mathbf{V}''_a - Z_{at} \mathbf{I}'_a \quad (4)$$

$$G'_a = \frac{1}{Z''_a Y_{ca} + 1} \quad (5)$$

$$Z_{at} = \frac{Z''_a}{Z''_a Y_{ca} + 1} \quad (6)$$

To complete the SAPF model, the transformer model shown in Fig. 4 is included. From Fig. 4 the following equations can be written:

$$\mathbf{V}'_a = Z'_a \mathbf{I}'_a + Z_m \mathbf{I}_g \quad (7)$$

$$\mathbf{V}_a = Z_a \mathbf{I}_g + Z_m \mathbf{I}'_a \quad (8)$$

Substituting (7) into (8) the following transformer transfer function are found :

$$\mathbf{V}_a = \frac{Z_m}{Z'_a} \mathbf{V}'_a + \frac{Z_a Z'_a - Z_m^2}{Z'_a} \mathbf{I}_g \quad (9)$$

$$\mathbf{I}'_a = \frac{\mathbf{V}'_a - Z_m \mathbf{I}_g}{Z'_a} \quad (10)$$

Finally, v_a as a function of v''_a is obtained by substituting (9) and (10) into (4), which results in

$$\mathbf{V}_a = \frac{Z_m}{Z'_a(Z''_a Y_{ca} + 1) + Z''_a} \mathbf{V}''_a + \frac{(Z_a Z'_a - Z_m^2)(Z''_a Y_{ca} + 1) + Z_a Z'_a}{Z'_a(Z''_a Y_{ca} + 1) + Z''_a} \mathbf{I}_g \quad (11)$$

This equation can also be written as

$$\mathbf{V}_a = G_a \mathbf{V}''_a + Z_{ga} \mathbf{I}_g \quad (12)$$

where

$$G_a = \frac{X_m}{Z'_a(Z''_a Y_{ca} + 1) + Z''_a} \quad (13)$$

$$Z_{ga} = \frac{(Z_a Z'_a - Z_m^2)(Z''_a Y_{ca} + 1) + Z_a Z'_a}{Z'_a(Z''_a Y_{ca} + 1) + Z''_a} \quad (14)$$

Analysis of (12), shows that Z_{ga} appears multiplied by \mathbf{I}_g . This implies Z_{ga} in series with Z_g , so that the equivalent impedance between source voltage and load is $Z_{gt} = Z_{ga} + Z_g$. The complete load voltage transfer function of SAPF is then rewritten from equation (3) as:

$$\mathbf{V}_l = -\frac{Z_l}{Z_{gt} + Z_l} G_a \mathbf{V}''_a + \frac{Z_l}{Z_{gt} + Z_l} \mathbf{E}_g \quad (15)$$

III. STEADY STATE

The steady state analysis determines the behavior of currents and voltages when the SAPF is in operation. Consequently, it is possible to manipulate the SAPF parameters to minimize the converter currents and voltages. Besides that, it is also possible to verify the source power factor behavior. That is important because the operation with a low source power factor results in a penalty for the customer.

This analysis is accomplished by writing the SAPF model, with all elements, in a complex form, and then solving the equations for the conditions bellow

$$v_{ld} = V_m \quad (16)$$

$$v_{lq} = 0 \quad (17)$$

$$P''_a = 0 \text{ (Converter active power)} \quad (18)$$

Subscript d stands for the real component and q stands for the imaginary component of the complex variable. Conditions (16)-(17) are employed to maintain the amplitude load voltage constant and v_{lq} is set to zero to simplify the equations. Condition (18) imposes the converter active power in steady-state. Solving the serie circuit model (Fig. 2) for conditions (16)-(18), a second order non-linear system, it is obtained as solution:

$$\begin{cases} k_{ast} i_{ad}^2 + k_{ast} i_{aq}^2 + k_{bst} i'_{ad} + k_{cst} i'_{aq} + k_{dst} = 0 \\ x_m^2 i_{ad}^2 + x_m^2 i_{aq}^2 + k_{8st} i'_{aq} + k_{9st} i'_{ad} + k_{10st} = 0 \end{cases} \quad (19)$$

where

$$\begin{aligned}
k_{ast} &= k_{4st}k_{1st} + k_{5st}k_{2st} \\
k_{bst} &= -a_l k_{4st}k_{3st} + k_{6st}k_{1st} - b_l k_{3st}k_{5st} + k_{2st}k_{7st} \\
k_{cst} &= a_l k_{5st}k_{3st} - k_{2st}k_{6st} - b_l k_{4st}k_{3st} + k_{1st}k_{7st} \\
k_{dst} &= -a_l k_{3st}k_{6st} - b_l k_{3st}k_{7st} \\
k_{1st} &= 1 - x'_a/x_{ca} \\
k_{2st} &= r'_a/x_{ca} \\
k_{3st} &= (x_m/x_{ca})V_m \\
k_{4st} &= -x''_a k_{2st} + r''_a k_{1st} + r'_a \\
k_{5st} &= +x''_a k_{1st} + r''_a k_{2st} + x'_a \\
k_{6st} &= -a_l r''_a k_{3st} + b_l x''_a k_{3st} - b_l x_m V_m \\
k_{7st} &= -a_l x''_a k_{3st} - b_l r''_a k_{3st} + a_l x_m V_m
\end{aligned}$$

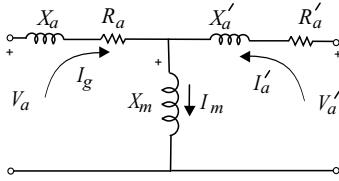


Fig. 4: Transformer model.

This system has no analytical solution, and the Newton-Raphson numerical method is used to solve it. Parameters used were: RL load of $S_l = 1750, 0VA$ PF = 0,7, and a voltage supply of $220V_{rms}$ source voltage. Other parameters are given in table 1

$r_g = 0,055\Omega$	$l_g = 1,5mH$	$l''_a = 1,5mH$	$l_m = 1H$
$r''_a = 1,6\Omega$	$c_a = 120\mu F$	$l_d = 0,1mH$	

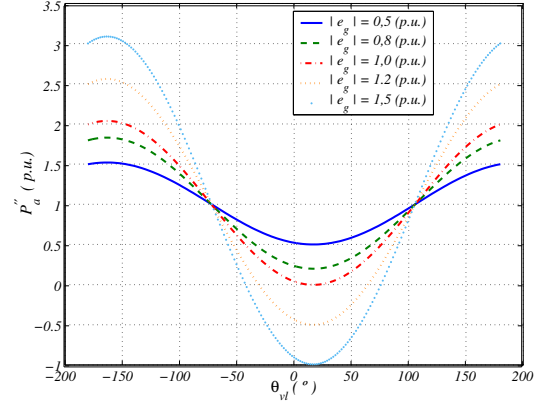
Table 1: Parameters of series active power filter.

To better understand these results, the parameters were transformed in *p.u.* bases, by using the source voltage and the load power as references. In this analysis only the fundamental frequency component is considered.

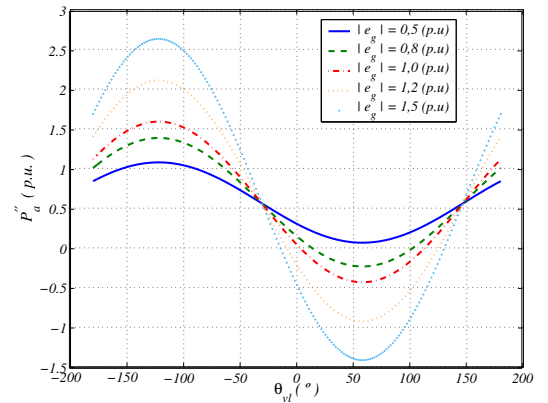
During simulation, it was verified that the active power converter is not null (condition (18) fail) for a low reactive load. This situation occurs in case of source voltage sag, as shown in Fig. 5(a) for $|e_g| < 1,0$ (*p.u.*). The solution is the point in which $P''_a = 0$, in Fig. 5. In this figure, it is observed that P''_a is always positive for $|e_g| < 1,0$ (*p.u.*), which implies that an external dc-link voltage is necessary to regulate the load voltage. This is one of the reasons of the use of DVRs with a coupled source supply.

However, it is possible to regulate the load voltage without an external source supply, in case of more reactive loads, as shown on Fig. 5(b). In this figure it is observed that for $|e_g| = 0,8$ (*p.u.*) have a solution for (19). In these cases the control strategy capable to compensate harmonics and to regulate the load voltage as well.

From the point of view of the source power factor, it is observed in Fig. 6 that the source power factor decreases



(a)



(b)

Fig. 5: Series converter power as a functions of θ_{vl} for, (a) $FP_{carga} = 0,95$, (b) $FP_{carga} = 0,5$.

as $|e_g|$ increases. It is also observed that less reactive load results in better source PF. The conclusion is that under source voltage swells the customer will be more exposed to penalties than under a voltage sag.

It is possible to minimize the voltage or current by manipulation of the transformer winding relation n ($n > 1$ implicate a gain from v'_a to v_a , and $n < 1$ implicate a attenuation). To verify the behavior of converter currents and voltage, it was made a variation of transformer magnetization inductance for three values of n . From Fig. 7(a) it is observed that the smallest current value was obtained for $n = 1$, the smallest voltage values where found for $n = 6$, as it is shown in Fig. 7(b). In this situation, the current behavior determines the choice of n , that is, $n = 1$.

In the situation shown in Fig. 7(a), i''_a isn't small for $n = 0.1$ than for $n = 1$ because of the capacitive impedance. The explanation is that v'_a with $n = 0.1$ is bigger than v'_a with $n = 1$, and since this is the capacitor voltage (see Fig. 3), the converter current for $n = 0,1$ is bigger than that for $n = 1$; if the capacitive impedance

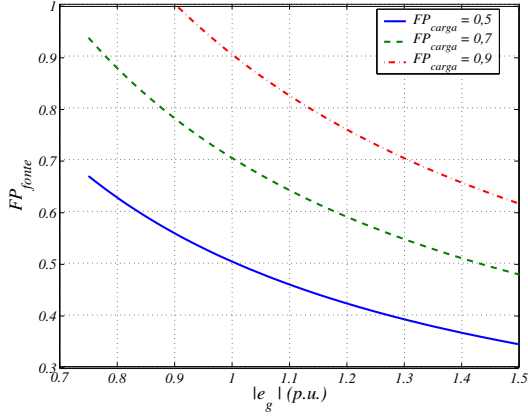


Fig. 6: Power factor as function of $|e_g|$.

is low, i_{ca} is high and, consequently, i_a'' is high too. This way, i_a'' is minimized for $n < 1$ by increase of x_{ca} , like is shown in Fig. 8. This form, it is preferable to work with a small capacitance.

IV. CONTROL STRATEGY

The control strategy for the SAPF is described by diagram block in Fig. 9. Such strategy allows to compensate the harmonic voltage and to regulate the load voltage. The controller must track a sinusoidal waveform reference, free of harmonics and with a constant amplitude. The phase of load voltage reference is determined by the controller R_c , that is responsible to maintain the dc bus voltage at a desirable value. This controller is implemented with a simple PI, and R_v includes a double sequency controller. The output R_v gives the reference voltage for the PWM modulation.

The pulse-width modulation can be determined directly from the grid and load voltages referred to the dc -bus mid-point, which in turn are defined from the desired reference phase voltages for grid and load. If the desired reference voltages are given by v_{a1}^* , v_{a2}^* and v_{a3}^* , then the voltages referred to the mid-point bus can be expressed as:

$$v_{a10}''^* = v_{a1}''^* + v_{n0}^* \quad (20)$$

$$v_{a20}''^* = v_{a2}''^* + v_{n0}^* \quad (21)$$

$$v_{a30}''^* = v_{a3}''^* + v_{n0}^* \quad (22)$$

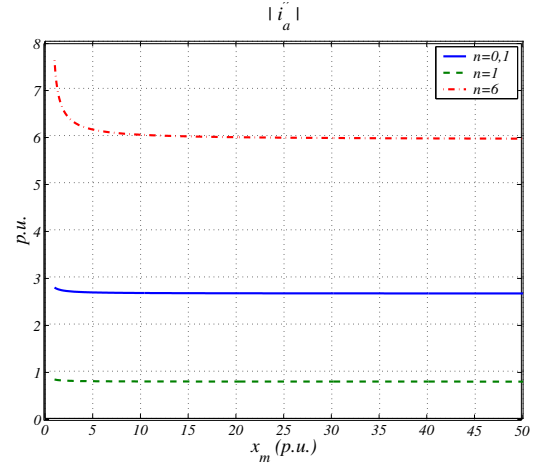
The voltage v_{n0}^* can be calculated based on the global apportioning factor μ , that is:

$$v_{n0}^* = E\left(\mu - \frac{1}{2}\right) - \mu v_{max}^* + (\mu - 1)v_{min}^* \quad (23)$$

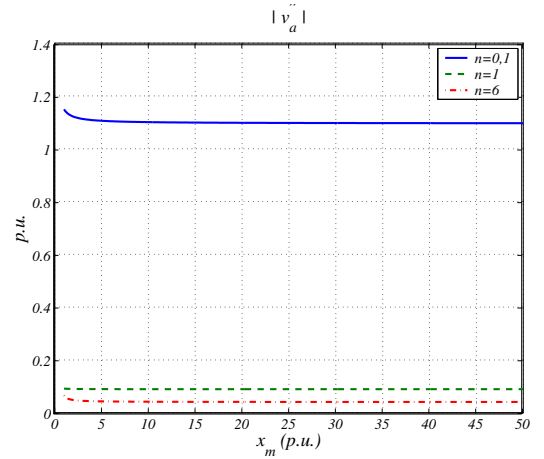
where $v_{max}^* = \max V$ e $v_{min}^* = \min V$, and $V = \{v_{a1}''^*, v_{a2}''^*, v_{a3}''^*\}$. This expression was derived by using the same approach as used to obtain the equivalent one for the three-phase *PWM* modulator [6].

The apportioning factor μ ($0 \leq \mu \leq 1$) is given by

$$\mu = t_{oi}/t_o \quad (24)$$



(a)



(b)

Fig. 7: (a) $|i_a''|$, (b) $|v_a''|$ as function of x_m and n .

and splits the free-wheeling period t_o at the beginning ($t_{oi} = \mu t_o$) and at the end ($t_{oe} = (1 - \mu)t_o$) of the switching period [6], [7]. The apportioning factor can be changed as a function of the modulation index (mi) to reduce the *THD* (total harmonic distortion) of the output voltage [6],[7]. In this case, the proposed algorithm is:

Step 1. Choose the global apportioning factor μ and calculate v_{n0}^* from (23).

Step 2. Determine v_{a10}^* , v_{a20}^* and v_{a30}^* from (20)-(22).

Step 3. Finally, once the mid-point voltage have been determined, calculate pulse-widths τ_{a1} , τ_{a2} , τ_{a3} by using

$$\tau_{aj} = \frac{T}{2} + \frac{T}{E} v_{aj0}^* \quad \text{for } j = 1, 2, 3 \quad (25)$$

where T , is the *PWM* switching period.

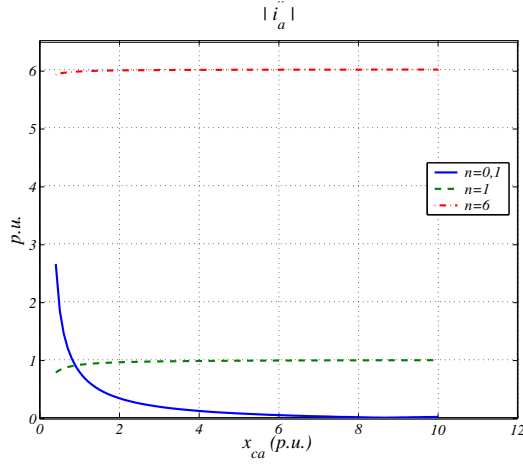


Fig. 8: $|i_a''|$ as function of x_{ca} and n .

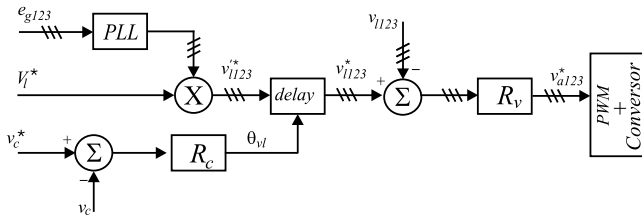


Fig. 9: Control block diagram of the system.

V. SIMULATION AND EXPERIMENTAL RESULTS

The simulation of the dynamic operation of the series active power filter system was developed by using the parameters of Table 1 and a dc bus with $2 * 220\sqrt{2}(V)$. To verify the controller action, a fifth harmonic was added to the source voltage (with a 15% of fundamental magnitude) in $t = 0.5s$, as shown in Fig. 10(a). In this figure, it is also shown the source current, which is not in phase with the voltage. In Fig. 10(b) it is shown the controlled load voltage, of which the calculated THD was 2.39%. Fig. 10(c) shows the compensation voltage of the transformer. To verify the load voltage regulation, a variation of $\pm 20\%$ was applied to source voltage. At $t=0.6s$ the magnitude of source voltage changes from 248.9(V) (-20%) to 373.35(V) (+20%), as shown in Fig. 11(a). Fig. 11(b) shows the regulated load voltage. The THD calculated was 0.72% in the case of voltage sag and 0.34% in the case of voltage swell. The transformer compensation voltage is shown in Fig. 11(c).

These results show that it was possible to operate with a load voltage amplitude regulated for the rated value reference. When the load and input voltage conditions do not allow operate with $P_a'' = 0$ then it is necessary to reduce the reference load voltage amplitude.

The experimental results were obtained with a three-phase RL load of 9,0 mH and 30 incandescent lamp of 100 W Y connected. They are showed in Fig. 12. In these results, the load voltage reference is a sinusoidal signal with amplitude of 100V, and the grid voltage amplitude

is 120V. Fig. 12(b) indicates the regulation load voltages. The DC bus was controlled at 200V as shown in Fig. 12(c).

VI. CONCLUSIONS

This paper presented a study of active serie power filter, based on the system modelling and steady state analysis. The system modelling was made so that the new transfer function can be easily obtained, in case of change structure. It was observed by steady state analysis that in some cases it is impossible to regulate the load voltage without a dc-link source. In cases in which it is possible to regulate the load voltage, the controller worked very well. When it is not possible to regulate the load voltage, the system allows to operate with the load voltage free of harmonics, even there are harmonics in the input voltage.

VII. ACKNOWLEDGEMENT

The authors would like to thank the financial support provided by the Conselho Nacional de Desenvolvimento Científico e Tecnológico (CNPq) and (CAPES) of Brazil.

REFERENCES

- [1] B. Singh, K. Al-Haddad, and A. Chandra. A review of active filters for power quality improvement. *IEEE Trans. Ind. Electron.*, 46(5):960–971, Oct. 1999.
- [2] H. Akagi. Active harmonics filters. *IEEE proceedings*, 93(12):625–630, dec 2005.
- [3] F. Z. Peng, H. Akagi, and A. Nabae. A new approach to harmonic compensation in power systems—a combined system of shunt passive and series active filters. *IEEE Trans. On Industry applications*, 26(6):983–990, Nov/Dec 1990.
- [4] weiMin Wu, Liqing Tong, Z. M. Qian, Zheng Yu Lu, and F. Z. Peng. A new control strategy for series type active power filter. *35th Annual IEEE Pow. Electr. Spec. Conf.*, 4, 2004.
- [5] E. R. Ribeiro and I. Barbi. Harmonic voltage reduction using a series active filter under different load conditions. *IEEE Trans. on power electr.*, 21(5):1394–1402, sept 2006.
- [6] C. B. Jacobina, A. M. N. Lima, E. R. C. da Silva, R. N. C. Alves, and P. F. Seixas. Digital scalar pulse width modulation: a simple approach to introduce non-sinusoidal modulating waveforms. *IEEE Trans. Power Electron.*, 16(3):351–359, May 2001.
- [7] V. Blasko. Analysis of a hybrid pwm based on modified space-vector and triangle-comparison methods. *IEEE Trans. Ind. Applicat.*, 33(3):756–764, May/June 1996.

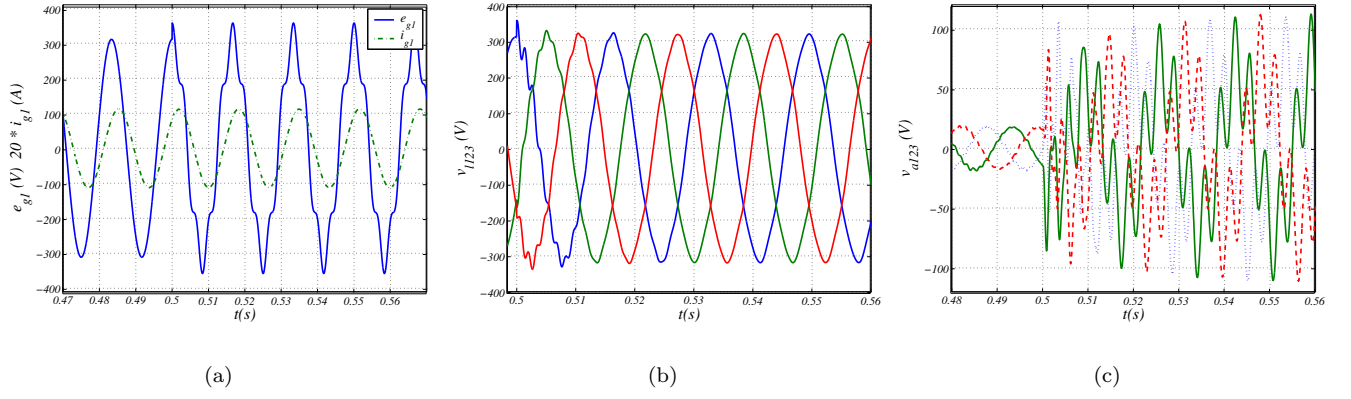


Fig. 10: Simulation results for harmonic in the source voltage. (a) Source voltage and current, (b) load voltage, (c) secondary transformer voltage.

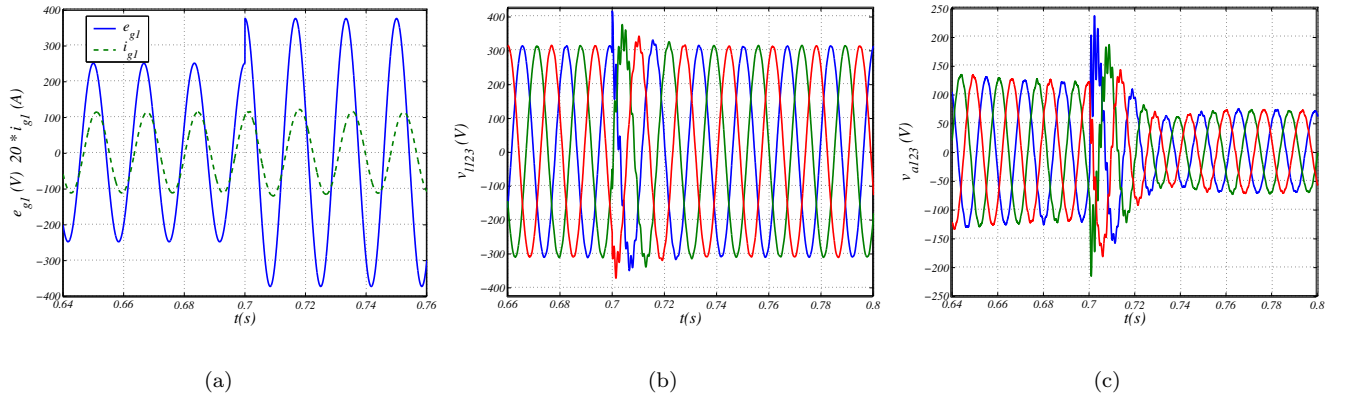


Fig. 11: Simulation results for variation of amplitude source voltage. (a) Source voltage and current, (b) load voltage, (c) secondary transformer voltage.

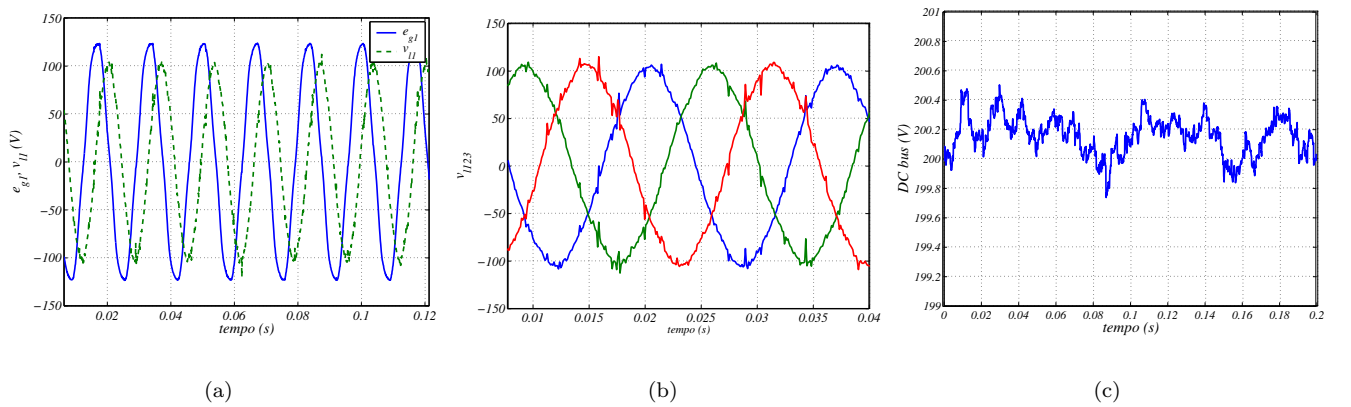


Fig. 12: Experimental results for variation of amplitude source voltage. (a) Source voltage and load voltage, (b) load voltage, (c) DC bus voltage.